

# Reliability of Segmenting Brain Tumor and Finding Optimal Volume Estimator for MR Images of Patients with Glioma's

T . Kalaiselvi, P. Kumarashankar, P. Sriramakrishnan

**Abstract:** Tumor volume estimation is a significant prognostic part of the Glioma tumor detection. Reliable assessment of Glioma tumor segmentation and volume estimation is a common problem in clinical aspects. We aim to propose a tumor segmentation method by suggesting suitable estimator for MR brain tumor volume construction. Run length algorithm is used to automatic initialize the seed point to the region growing algorithm. Region growing algorithm works with a threshold value using  $8 \times 8$  patches. In this experiment includes thirty BraTS2013 high-grade and low-grade Glioma datasets. Proposed method yield 80.12% of Dice similarity with 6.8% of deviation and 84% of accuracy with 10% of deviation. The proposed work uses six state-of-the-art volume detectors to estimate the size of tumor volume. From the results, Cavalieri's estimator gives more accurate results with less deviation.

**Index Terms** Volume estimators, Rectangular estimator, Cavalieri's Estimator, Trapezoidal Estimator, Parabolic Estimator, Truncated Pyramid, Simson's Estimators

## I. INTRODUCTION

Computer-aided diagnosis is the interpretation of medical images by automatic systems that assist the doctors in diagnosing a particular disease. There are various types of imaging available in the medical industry that includes X-ray, ultrasound scans, computed tomography (CT), magnetic resonance imaging (MRI), etc. These imaging systems present a detailed structure of the human organs and are to be interpreted by the doctors to analyze and understand the problems/abnormalities in the anatomical structure of the human body [1]. Given that the time is very short for evaluation and the accuracy of the diagnosis, computer systems can help the physicians in evaluating these images and recommended the diagnostic process.

For brain-related diseases, MRI is the safest imaging modalities suggested by the clinicians to diagnose abnormalities. MRI gives detailed information about the soft tissue characteristics [2]. It is the most commonly used imaging technique for monitoring and evaluating brain tumors..

**Revised Manuscript Received on July 05, 2019.**

**Kalaiselvi T.** currently working as an Assistant Professor in Department of Computer Science and Applications, Gandhigram Rural Institute – Deemed University, Dindigul, India.

**Kumarashankar P.** is currently working as a Project Manager with a leading IT MNC. He received his Bachelor of Science (Computer Science) degree from Madurai Kamaraj University, Madurai, Tamil Nadu India

**Sriramakrishnan P.** is a Research Scholar (Full-time) in the Department of Computer Science and Applications, Gandhigram Rural Institute - Deemed University, Dindigul, India.

MR scanner follows nuclear magnetic resonance (NMR)

principle by using strong magnetic and radio frequency MR scanner provides various characteristics of brain images such as T1-weighted, T1-weighted contrast enhancement (T1c), T2-weighted and FLAIR (fluid attenuated inversion rejection) based on repetition time (TR) and echo time (TE).

A brain tumor is an abnormal unpredictable cells development in the brain. There are different types of tumors that exist namely benign and malignant. Benign cells are non-cancerous whereas malignant tumors are cancerous [3]. Tumors can begin in other parts of the body and then spread to the brain which is called secondary. The tumor growth rate varies from case to case and how it will impact the functions of the nervous system is subjective. Developing methods for automatic segmentation of brain tumor is an emerging field. Manual segmentation requires more time and has increase rate of error [4]. Past few decades, machine learning and deep learning algorithms play an important role in segmentation. Tumor volume is used to evaluate the disease progression, treatment response, and need for changes in treatment plans [5]. Volume estimation can help to visualize the tumor which tells the exact characteristic and size of the tumor. The tumor size in 3D view plays an important role in the successful diagnosis and treatment plan. Generally, tumor volume is measured in the unit of a millimeter ( $\text{mm}^3$ ) or centimeter ( $\text{cm}^3$ ). Several methods have been proposed for brain tumor segmentation and volume estimation [6]. Abdulbaq et al. proposed a method for segmenting brain tumor and volume size estimation using hidden Markov random field-expectation maximization (MRF-EM) on CT images [7]. Mango software is used to measure the tumor volume. Ficici et al. developed a method for finding brain tumor and estimating volume using FLAIR and T1C MR images [8]. Bilateral symmetrical property helps to detect the abnormal images and thresholding, skull stripping and fuzzy c mean (FCM) clustering pipeline operations are used to segment the tumor region. Tumor volume is calculated from dataset information that can be obtained from the DICOM header. Shoaib and Ajaz developed a system for brain tumor segmentation and volume estimation by statistical texture feature map and active contour [9].

Then Surveyor's algorithm is used to compute



the volume of tumors. The accuracy of the volume is compared with famous ABC/2 method and Cavalieri method.

In this current work, we have aimed to propose a tumor segmentation method and suggest a suitable estimator for MR brain tumor volume construction. Brain tumor segmentation is done by using run-length based region growing technique. Run length algorithms initialize the region growing algorithm and works with a threshold value on  $8 \times 8$  patches. In this experiment, thirty BraTS2013 high-grade and low-grade Glioma dataset are used. The proposed work uses eight state-of-the-art volume detectors to estimate the volume size of tumors namely Rectangular estimator, Cavalieri's estimator, Trapezoidal estimator, Parabolic estimator, Simpson's 3/8 estimator, Durand's estimator. These estimators are capable of estimating the regular and irregular shape of tumor volume. From our analysis, Cavalieri's estimator gives more accurate results with less deviation.

## II. METHODOLOGY

Proposed method contains two stages: tumor segmentation and volume estimation. Block diagram of the proposed method is shown in Fig. 1. Tumor images are input for the proposed system.

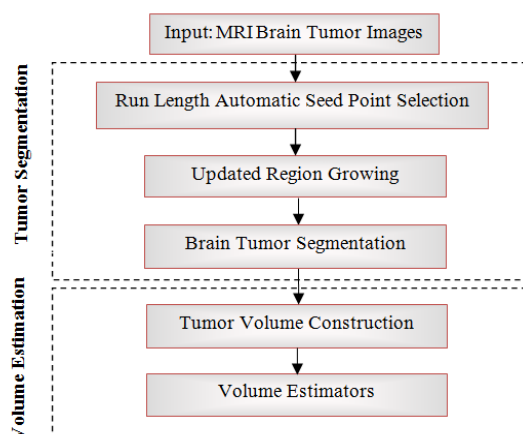


Fig. 1: Block diagram of the proposed method

### A. Brain Tumor Segmentation

The proposed method automatically selects the seed point using run length method. Automatic seed point has been selected from the highest occurrence of the maximum intensity found in an image. This procedure is followed as the tumor appearance in T2 image have the maximum intensity as shown in Fig. 2. This seed point is given as input to updated region growing technique for tumor segmentation.

This novel updated region growing technique uses a threshold value which can be obtained from a mean intensity of  $8 \times 8$  patches of seed pixel. Patch is a small unit of brain image that helps to decide segmentation and is shown in Fig. 2. Threshold determines whether neighbor patch can be merged into seed point or split into  $4 \times 4$  smaller patches based on the minimum or maximum intensities in each patch. If min-max difference was less than the threshold, then the patches are merged into a single. A patch is split in half if the min-max difference is greater than the threshold. This process

is continued until, no patch satisfies the criteria to merge and split.

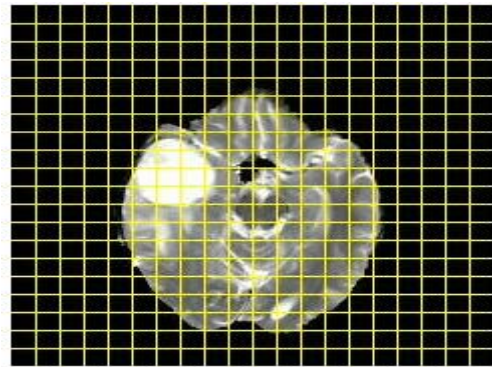


Fig. 2: MR brain image with  $8 \times 8$  patch

### B. Tumor Volume Estimation

In stage 2, qualitative and quantitative post-processing validation is done by tumor volume construction and estimation respectively. Tumor volume construction can visualize the tumor volume in the 3D form which may help the physician to understand the aggressiveness of the tumor. For clinical follow-up, tumor volume is essential. Volumetric assessment of tumor with manual segmentation is a time – consuming process that can be overcome by automatic computerized methods.

The volume of tumor is measured in the unit of  $\text{cm}^3$  or  $\text{mm}^3$  of voxels. Varieties of estimators are available to measure the volume of the tumor namely Rectangular estimator, Cavalieri's estimator, Trapezoidal estimator, Parabolic estimator, Simpson's 3/8 estimator, and Durand's estimator [10]. In continuation, a suitable estimator for brain tumor volume calculation is identified using proposed segmentation results. The following subsections in this paper explain these estimators in detail.

#### Rectangular Estimator

Rectangular estimator is calculated using Eqn. (1).

$$V_R = d \sum_{i=1}^{n-1} (y_i) \quad (1)$$

where,  $d$  distance between the sections (inter-slice gap),  $y_i$  cross-sectional area of the  $i^{\text{th}}$  section through the morphometric region and  $n$  number of sections.

#### Cavalieri's Estimator

Cavalieri's Estimator is more accurate with equally spaced section. It is a statically unbiased form of rectangular approach which requires systematic sampling and defined ( $V_c$ ) in Eqn. (2).

$$V_c = d \left[ \sum_{i=1}^n y_i \right] - (t)y_{max} \quad (2)$$

where,  $y_{max}$  – maximum value of  $Y$ ,  $t$  – section thickness.

#### Trapezoidal Estimator

Trapezoidal estimator is an enhanced method of rectangular approximation

and determined by the following formula:

$$V_T = d \left[ \frac{1}{2} (y_1 + y_n) + y_2 + y_3 + \dots + y_{n-1} \right] \quad (3)$$

#### Parabolic Estimator

Parabolic estimator is an improved version of Trapezoidal estimators and defined as:

$$V_P = \frac{d}{3} [(y_1 + y_n) + 4(y_2 + y_4 + \dots + y_{n-1}) + 2(y_3 + y_5 + \dots + y_{n-2})] \quad (4)$$

where, the total number of sections (n) is required to be odd.

#### Simpson's 3/8 Estimator

Simpson's can estimate the area under a curve with an even numbering of sections using either a modification of Simpson's 3/8 rule and given in Eqn. (5).

$$V_S = \frac{d}{3} [(y_1 + y_{n-3}) + 4(y_2 + y_4 + \dots + y_{n-4}) + 2(y_3 + y_5 + \dots + y_{n-5}) + \frac{3}{8}(y_{n-3} + 3(y_{n-2}) + 3(y_{n-1}) + y_n)] \quad (5)$$

#### Durand's Estimator

Durand's estimator will work on odd or even number of section available in the volume but it requires equal space between the sections and defined in Eqn. (6).

$$V_D = d[0.4(y_1 + y_n) + 1.1(y_2 + y_{n-1}) + y_3 + y_4 + \dots + y_{n-2}] \quad (6)$$

### III. RESULTS AND DISCUSSION

The experiment is carried out in systems with the configuration of 1.73 GHz Intel i3 processor, 2 GB RAM and Windows 7 operating system. Twenty Glioma tumor datasets were collected from the virtual skeleton database (VSD) which contains multi-sequence MR scans and gold standard results given by experts and named as brain tumor segmentation (BraTS2013) [11]. The datasets include high-grade and low-grade gliomas (HGGs and LGGs). Images in the dataset were registered to a common space, re-sampled to  $1\text{mm} \times 1\text{mm} \times 1\text{mm}$  resolution and image dimensions of  $240 \times 240 \times 155$  voxels.

Qualitative result of proposed segmentation is shown in Fig.3. The first column shows the original images, the second column denotes segmented obtained image by the proposed method, the third column means actual image given by experts. The proposed method works well in multimodal images (FLAIR and T2) available in the BraTS2013 dataset. Qualitatively, the current method gives the closest result with the actual result. In quantitative analysis, the current method yield 80.12% of Dice accuracy with 6.8% of deviation and 84% of accuracy with 10% of deviation. This segmented result shows that the proposed method works well and good in both HGG and LGG Glioma segmentation.

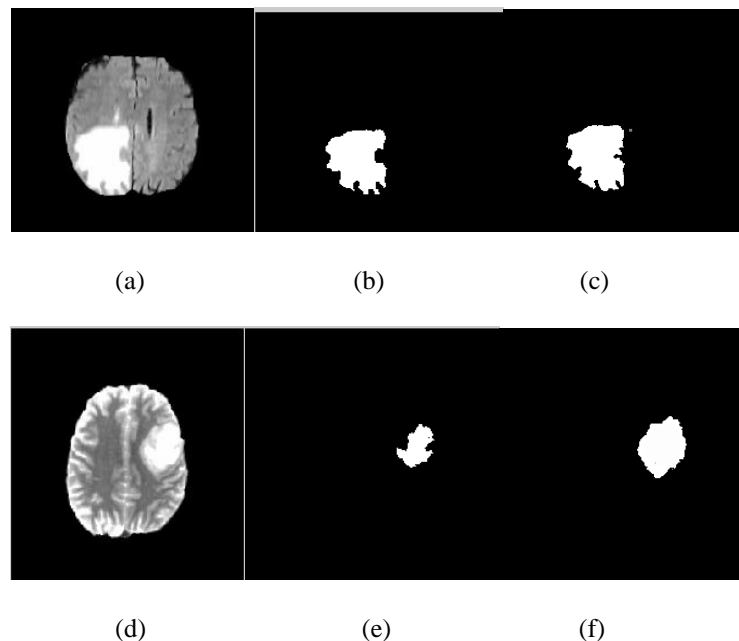


**Fig. 3. Qualitative results of the proposed method on BraTS2013. (a) HGG FLAIR image (b) Segmented image (c) Gold standard image (d) LGG T2 image (e) Segmented image (f) image (c) Gold standard image**

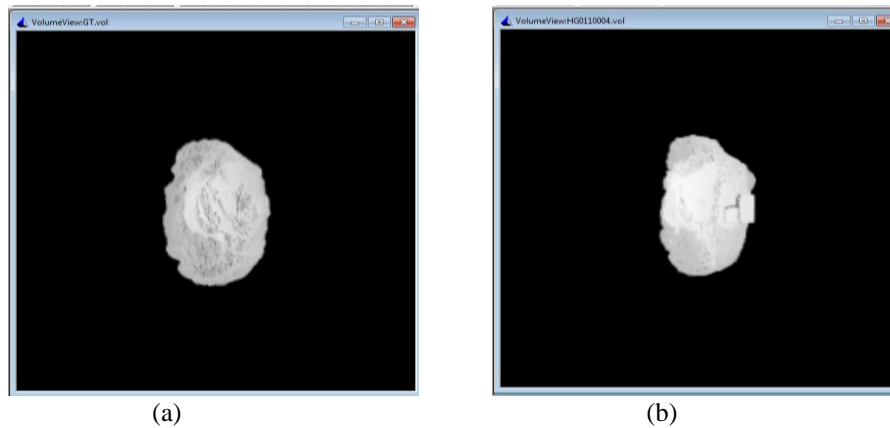


Fig. 4: Tumor volume construction (a) Actual tumor volume given by the experts (b) Obtained tumor volume by the current method

Table 1: Quantitative results of volume estimation on actual tumor volume ( $\text{mm}^3$ )

| No . | Volume Name | Rectangular Estimator | Cavalieri Estimator | Trapezoidal Estimator | Parabolic Estimator | Simpson Estimator | Durand's Estimator |
|------|-------------|-----------------------|---------------------|-----------------------|---------------------|-------------------|--------------------|
| 1    | HG0001      | 112856                | 110369              | 112978.5              | 0                   | 114554.2          | 113023.7           |
| 2    | HG0002      | 59566                 | 58108               | 59452.5               | 0                   | 59564.46          | 59466.8            |
| 3    | HG0003      | 119149                | 117284              | 119660                | 119256              | 117891.6          | 119676.8           |
| 4    | HG0004      | 101808                | 99609               | 101832.5              | 0                   | 102612.8          | 101844.6           |
| 5    | HG0005      | 57278                 | 56339               | 56808.5               | 56949.67            | 55818.13          | 56773.2            |
| 6    | HG0006      | 172916                | 168487              | 172860.5              | 0                   | 173466.3          | 172912.4           |
| 7    | HG0007      | 68473                 | 65910               | 67191.5               | 0                   | 67501.58          | 67216.8            |
| 8    | HG0008      | 185445                | 181953              | 184745                | 184819.3            | 183896.8          | 184710.4           |
| 9    | HG0009      | 166963                | 163385              | 166733.5              | 167117              | 165811            | 166760.6           |
| 10   | HG0010      | 15497                 | 15403               | 15574                 | 15671.33            | 13548.38          | 15593              |
| 11   | HG0011      | 123435                | 120593              | 123437.5              | 123335              | 122565.8          | 123465.5           |
| 12   | HG0012      | 19034                 | 18607               | 18948                 | 0                   | 18827.21          | 18933.5            |
| 13   | HG0013      | 13949                 | 13482               | 13814                 | 13805.33            | 13042             | 13825.1            |
| 14   | HG0014      | 155223                | 151735              | 153802                | 0                   | 154825.3          | 153613             |
| 15   | HG0015      | 141175                | 137582              | 140692                | 141520              | 140851.6          | 140726.5           |
| 16   | HG0022      | 101600                | 101573              | 103137.5              | 0                   | 102872.4          | 103151.7           |
| 17   | HG0024      | 105294                | 102645              | 104202.5              | 104060.3            | 101416.5          | 104225.1           |
| 18   | HG0025      | 86856                 | 85082               | 86616.5               | 0                   | 86626.67          | 86634.8            |
| 19   | HG0026      | 66762                 | 63963               | 66808                 | 0                   | 66110.92          | 66787.5            |
| 20   | HG0027      | 126336                | 121890              | 124862                | 0                   | 124846.2          | 124849.9           |
| 21   | LG0001      | 29126                 | 26511               | 29377.5               | 0                   | 30226.33          | 29380.2            |
| 22   | LG0002      | 210553                | 206461              | 210561.5              | 0                   | 210825.7          | 210598.2           |
| 23   | LG0004      | 47919                 | 46747               | 47705                 | 47372.67            | 45843.46          | 47652.2            |
| 24   | LG0006      | 27177                 | 24377               | 25979.5               | 26197               | 25399.17          | 26073              |
| 25   | LG0008      | 32377                 | 30900               | 31726                 | 31796.67            | 30388.17          | 31723.4            |
| 26   | LG0011      | 51841                 | 50669               | 51523.5               | 0                   | 51560.25          | 51543.8            |
| 27   | LG0012      | 42178                 | 41141               | 42680                 | 42823.33            | 40775.29          | 42709.1            |
| 28   | LG0013      | 72130                 | 70001               | 72031                 | 0                   | 72767.21          | 72043.9            |
| 29   | LG0014      | 20429                 | 18878               | 20566                 | 20331.33            | 19319.5           | 20586.7            |
| 30   | LG0015      | 29309.5               | 28856               | 29309.5               | 29325.67            | 28572             | 29319.9            |
| AVG  |             | 85421.82              | 83284.67            | 85187.2               | 37479.3             | 84744.23          | 85194.04           |



Table 2: Quantitative results of volume estimation on proposed method (mm<sup>3</sup>)

| No.        | Volume Name | Rectangular Estimator | Cavalieri Estimator | Trapezoidal Estimator | Parabolic Estimator | Simpson Estimator | Durand's Estimator |
|------------|-------------|-----------------------|---------------------|-----------------------|---------------------|-------------------|--------------------|
| 1          | HG0001      | 108790                | 106424              | 108795                | 0                   | 109087.2          | 108805.7           |
| 2          | HG0002      | 48677                 | 47304               | 48671                 | 48738.67            | 48576.83          | 48674.6            |
| 3          | HG0003      | 153561                | 150309              | 153570                | 153684.7            | 153443.5          | 153575             |
| 4          | HG0004      | 106722                | 104350              | 106737                | 0                   | 106671.1          | 106745.4           |
| 5          | HG0005      | 60173                 | 58871               | 60148                 | 0                   | 60170.58          | 60167              |
| 6          | HG0006      | 179702                | 175680              | 179704                | 179844              | 179068.7          | 179717.3           |
| 7          | HG0007      | 88254                 | 85147               | 88268.5               | 0                   | 88321.63          | 88276.6            |
| 8          | HG0008      | 200092                | 195691              | 200099.5              | 200053              | 199746            | 200108             |
| 9          | HG0009      | 219073                | 214705              | 219193.5              | 219429.7            | 218133.8          | 219219.8           |
| 10         | HG0010      | 15925                 | 15217               | 15928                 | 15926.67            | 15733.58          | 15936.7            |
| 11         | HG0011      | 144279                | 141227              | 144340.5              | 0                   | 144596.2          | 144351.5           |
| 12         | HG0012      | 20615                 | 19742               | 20605                 | 0                   | 20607.29          | 20610.8            |
| 13         | HG0013      | 10823                 | 10286               | 10849                 | 10855.33            | 10654.75          | 10859.2            |
| 14         | HG0014      | 141369                | 138077              | 141356                | 0                   | 141263.5          | 141376.8           |
| 15         | HG0015      | 180942                | 176493              | 180856                | 0                   | 180606.8          | 180866.4           |
| 16         | HG0022      | 84591                 | 82328               | 84570.5               | 84582.33            | 84246.25          | 84581.4            |
| 17         | HG0024      | 83623                 | 81158               | 83613                 | 0                   | 83754.13          | 83630.2            |
| 18         | HG0025      | 111532                | 108614              | 111478.5              | 0                   | 111662.4          | 111508.2           |
| 19         | HG0026      | 121670                | 121495              | 123204                | 0                   | 122524            | 122903.8           |
| 20         | HG0027      | 121537                | 118293              | 121536.5              | 121246.3            | 120982            | 121547.2           |
| 21         | LG0001      | 30672                 | 29854               | 30763                 | 30690               | 30043.88          | 30783.6            |
| 22         | LG0002      | 241684                | 236312              | 241707                | 241807.3            | 241117.5          | 241732.6           |
| 23         | LG0004      | 58873                 | 57339               | 58968                 | 59042               | 58539.71          | 58978.2            |
| 24         | LG0006      | 22468                 | 21649               | 22508                 | 0                   | 22468.38          | 22512.4            |
| 25         | LG0008      | 24737                 | 23736               | 24702.5               | 24724.33            | 24191.42          | 24757.5            |
| 26         | LG0011      | 53171                 | 51726               | 53178                 | 0                   | 53175.58          | 53203.7            |
| 27         | LG0012      | 42725                 | 41036               | 42701                 | 42728.67            | 42262.5           | 42708.1            |
| 28         | LG0013      | 77419                 | 75106               | 77394                 | 0                   | 77509.63          | 77421.3            |
| 29         | LG0014      | 16359                 | 15459               | 16344.5               | 16265               | 15855.75          | 16353.7            |
| 30         | LG0015      | 34808                 | 33645               | 34817.5               | 34863               | 34313.54          | 34838.2            |
| <b>AVG</b> |             | <b>93495.53</b>       | <b>91242.43</b>     | <b>93553.57</b>       | <b>49482.7</b>      | <b>93310.94</b>   | <b>93558.36</b>    |

Tumor volume construction is an essential task after segmentation which helps to visualize the tumor location, size and aggressiveness. Volume construction requires several parameters such as segmented tumor images in 2D, inter-slice gap, size of the images, and type of rendering. Volume construction is done through the 3D Doctor software [12]. Qualitative result of volume rendering is shown in Fig. 4. Tumor volume visualizes in 3D form give an accuracy of the proposed method. Figure 4 shows that the actual and obtained results are almost similar to each other.

Quantitative results of volume construction estimate by various volume estimators are given in Table 1 and Table 2. Table 1 shows the results of tumor volume for the gold standard in  $\text{mm}^3$ . Table 2 shows the results of tumor volume obtained by the proposed method. Seven volume estimators are used between actual and obtained tumor volume. From the tables, the results show that obtained tumor volume in size is less than actual tumor volume. This under estimation is due to 20% of segmentation loss, measured by the Dice metrics. Segmentation loss occurs because the current method has some difficulty to extract the edema region around the tumor (Fig. 3 (d) and (e)).

Comparison of estimator's results on actual and obtained tumor volume is consolidated in Table 3 with deviation. All the six estimators give around the same except parabolic estimator because parabolic estimator is computed when the volume has an odd number of slices. The volume has even number of slices omitted. Among the remaining five estimators, Cavalieri estimator is the best with less error rate in  $\text{mm}^3$  and yield maximum accuracy.

For systematic sampling, the rectangular method is not suitable and Cavalieri's estimator is the best one especially for irregular brain regions [6]. These results conclude that the Cavalieri's estimator is the best suitable method for brain volume estimation.

Table 3: Comparison of volume estimators

| Estimator Name        | Actual Tumor ( $\text{mm}^3$ ) | Obtained Tumor ( $\text{mm}^3$ ) | Deviation ( $\text{mm}^3$ ) |
|-----------------------|--------------------------------|----------------------------------|-----------------------------|
| Rectangular Estimator | 93495.5<br>3                   | 85421.82                         | 8073.71                     |
| Cavalieri Estimator   | 91242.4<br>3                   | 83284.67                         | 7957.76                     |
| Trapezoidal Estimator | 93553.5<br>7                   | 85187.2                          | 8366.37                     |
| Parabolic Estimator   | 49482.7                        | 37479.3                          | 12003.4                     |
| Simpson Estimator     | 93310.9<br>4                   | 84744.23                         | 8566.71                     |
| Durand's Estimator    | 93558.3<br>6                   | 85194.04                         | 8364.32                     |

## IV. CONCLUSION

This current work resolved a reliable assessment of Glioma tumor segmentation and volume estimation. This work also suggests suitable volume estimator for brain tumor volume estimation. Run length and region growing algorithms are used to segment the tumor region with the help of  $8 \times 8$  patches. The proposed method gave 80.12% of Dice similarity with 6.8% of deviation on BraTS2013 dataset. Finally, this paper concludes that the Cavalieri's estimator gives more accurate results with less deviation.

## REFERENCES

1. Prince, J. L., & Links, J. M. (2006). Medical imaging signals and systems. Upper Saddle River, NJ: Pearson Prentice Hall.
2. Rodger, J. A. (2015). Discovery of medical Big Data analytics: Improving the prediction of traumatic brain injury survival rates by data mining Patient Informatics Processing Software Hybrid Hadoop Hive. *Informatics in Medicine Unlocked*, 1, 17-26.
3. Sriramakrishnan, P., Kalaiselvi, T., & Rajeswaran, R. (2019). Modified local ternary patterns technique for brain tumour segmentation and volume estimation from MRI multi-sequence scans with GPU CUDA machine. *Biocybernetics and Biomedical Engineering*, 39(2), 470-487.
4. Kalaiselvi, T., Sriramakrishnan, P., & Somasundaram, K. (2017). Survey of using GPU CUDA programming model in medical image analysis. *Informatics in Medicine Unlocked*, 9, 133-144.
5. Liu, J., Udupa, J. K., Odhner, D., Hackney, D., & Moonis, G. (2005). A system for brain tumor volume estimation via MR imaging and fuzzy connectedness. *Computerized Medical Imaging and Graphics*, 29(1), 21-34.
6. Clark, M. C., Hall, L. O., Goldgof, D. B., Velthuizen, R., Murtagh, F. R., & Silbiger, M. S. (1998). Automatic tumor segmentation using knowledge-based techniques. *IEEE transactions on medical imaging*, 17(2), 187-201.
7. Abdulbaqi, H. S., Jafri, M. Z. M., Omar, A. F., Mutter, K. N., Abood, L. K., & Mustafa, I. S. B. (2015, December). Segmentation and estimation of brain tumor volume in computed tomography scan images using hidden Markov random field Expectation Maximization algorithm. In *2015 IEEE Student Conference on Research and Development (SCORED)* (pp. 55-60). IEEE.
8. Fiçici, C. Ö., Eroğlu, O., & Telatar, Z. (2017). Fully Automated Brain Tumor Segmentation and Volume Estimation Based on Symmetry Analysis in MR Images. In *CMBEBIH 2017* (pp. 53-60). Springer, Singapore.
9. Bandy, S. A., & Mir, A. H. (2017). Statistical textural feature and deformable model based brain tumor segmentation and volume estimation. *Multimedia Tools and Applications*, 76(3), 3809-3828.
10. Rosen, G. D., & Harry, J. D. (1990). Brain volume estimation from serial section measurements: a comparison of methodologies. *Journal of neuroscience methods*, 35(2), 115-124.
11. BraTS2013, <https://www.smir.ch/BRAITS/Start2013>
12. 3D Doctor, Software purchased under DST project sanction, Principle Investigators, Dr. T. Kalaiselvi, Department of Computer Science and Applications, Gandhigram Rural Institute.

## AUTHORS PROFILE



**Kalaiselvi T.** currently working as an Assistant Professor in Department of Computer Science and Applications, Gandhigram Rural Institute – Deemed University, Dindigul, India. She received her Bachelor of Science (B.Sc.) degree in Mathematics and Physics in the year 1994 and Master of Computer Applications (MCA) degree in the year 1997 from Avinashilingam University, Coimbatore. She received her Ph.D. (Full-time) degree from Gandhigram Rural Institute in the year

2010. In the year 2008, she received a project from Department of Science and Technology (DST), Government of India under Scheme for Young Scientists and Professionals (SYSP) by Science for Equity, Empowerment and Development (SEED) Division for three years (2008-2011). Her research focuses on Brain Image Processing and brain tumor or



lesion detection from MR Head Scans to enrich the Computer Aided Diagnostic process, Telemedicine and Tele radiology services. She is Academic Community Member (ACM) in International Congress for Global Science and Technology (ICGST), Life Member (LM) in Indian Society for Technical Education (ISTE) and Lifetime Member (LM) in Telemedicine Society of India (TSI).



**Kumarashankar P.** is currently working as a Project Manager with a leading IT MNC. He received his Bachelor of Science (Computer Science) degree from Madurai Kamaraj University, Madurai, Tamilnadu in the year of 2001. He received his Master of Computer Applications degree from the Gandhigram Rural Institute - Deemed University, Dindigul,

Tamilnadu in the year of 2004. He started his career as a software engineer and has got 15 years of IT industrial experience. He has good working experience in Banking and Insurance industry. His research focuses on Medical Image Processing. He has qualified for UGC NET in the year June 2012.



**Sriramakrishnan P.** is a Research Scholar (Full-time) in the Department of Computer Science and Applications, Gandhigram Rural Institute - Deemed University, Dindigul, India. He received his Bachelor of Science (B.Sc.) degree in 2011 from Bharathidasan University, Trichy, Tamilnadu, India. He received Master of Computer Application (M.C.A) degree in 2014

from Gandhigram Rural Institute- Deemed University, Dindigul, Tamilnadu, India. He worked as Software Developer in Dhvani Research and Development Pvt. Ltd, Indian Institute of Technology Madras Research Park, Chennai during May 2014 – March 2015. He is currently pursuing Ph.D. degree in Gandhigram Rural Institute- Deemed University. His research focuses on Medical Image Processing and Parallel Computing. He has qualified UGC-NET for Lectureship in June 2015.